

# Molecular dynamics simulation of plastic deformation of nanotwinned copper

A. J. Cao<sup>a)</sup> and Y. G. Wei<sup>b)</sup>

State Key Laboratory of Nonlinear Mechanics, Institute of Mechanics, Chinese Academy of Sciences, Beijing 100080, People's Republic of China

(Received 21 May 2007; accepted 17 August 2007; published online 17 October 2007)

The plastic deformation of polycrystalline Cu with ultrathin lamella twins has been studied using molecular dynamics simulations. The results of uniaxial tensile deformation simulation show that the abundance of twin boundaries provides obstacles to dislocation motion, which in consequence leads to a high strain hardening rate in the nanotwinned Cu. We also show that the twin lamellar spacing plays a vital role in controlling the strengthening effects, i.e., the thinner the thickness of the twin lamella, the harder the material. Additionally, twin boundaries can act as dislocation nucleation sites as they gradually lose coherency at large strain. These results indicate that controlled introduction of nanosized twins into metals can be an effective way of improving strength without suppression tensile ductility. © 2007 American Institute of Physics. [DOI: [10.1063/1.2794884](https://doi.org/10.1063/1.2794884)]

## I. INTRODUCTION

Recent studies have shown that both bulk ultrafine-grained (UFG) materials and one-dimensional (1D) metallic nanowires with nanosized twin structures exhibit ultrahigh strength.<sup>1-9</sup> This suggests that unique plastic deformation mechanisms are expected to be associated with the nanosized twin structures which are not seen in their coarse-grained (CG) counterparts. In order to explore the superior mechanical properties of these materials, studies on the twin structure hardening mechanisms have received considerable attentions recently.<sup>5-11</sup> However, despite previous encouraging experimental investigations, there are some related topics which are not well understood so far and need to be investigated in depth. For example, what is the role of twin boundaries (TBs) during deformation? Does the thickness of the twin lamella play a role in the strengthening effects? Interestingly and importantly, why the strength is enhanced without sacrificing tensile ductility compared with the CG counterparts? To gain insight into these fundamental issues, understanding of the detailed deformation mechanisms and the mechanical characteristics associated with these nanosized twins is demanded.

Molecular dynamics (MD) simulations have been used extensively in the past several years to study the plastic deformation of nanocrystalline (nc) materials.<sup>12-23</sup> Specifically, MD simulations have shown that the effect of growth twins on the plastic deformation mechanisms is different for several face-centered-cubic (fcc) metals, such as Cu, Ni, and Al.<sup>12,13</sup> The difference was attributed to the different ratios of the extrema of the generalized planar fault curves.<sup>12</sup> However, the effect of TBs on the mechanical properties has not been reported by using MD simulations until now. In the present paper, MD simulations are used to study the plastic

deformation of the nc Cu with ultrathin lamella growth twins, special attention is paid to elucidate the deformation mechanisms related to the TB interface.

## II. MD SIMULATION

Here a textured  $\langle 110 \rangle$  columnar microstructure is selected for simulation as the case in the experimental specimen.<sup>1,5-7</sup> We emphasize that this texture geometry is consistent with the experimental specimen with an evident  $(110)$  texture.<sup>5-7</sup> The simulation cell is consisted of four columnar, hexagonal grains that are rotated with respect to each other about the  $[1\bar{1}0]$  texture (or tilt) axis which defines the  $Z$  direction. Also because of the quasi-two-dimensional geometry, a few lattice planes are required to be considered in the periodically repeated texture direction, which enable us to simulate relatively large grain. For simplicity, the misorientation angles for the other three grains are chosen as  $60^\circ$ ,  $30^\circ$ , and  $90^\circ$ . In the texture ( $Z$ ) direction, the simulation cell contains 16  $(1\bar{1}0)$  planes, resulting in an initial  $Z$  thickness of 2.45 nm. The selected columnar microstructure is identical to the one used by Yamakov *et al.*<sup>23</sup> The detailed analysis of the microstructure can be found therein.

For comparison, three samples with same grain size of 35 nm are considered in the present work. In samples I and II, coherent growth twins are introduced within the grains. The twin lamella spacing (TLS)  $D_T$ , in the direction perpendicular to the TBs, is 3.1 nm in sample I and 11.3 nm in sample II, respectively. Sample III is twin-free in the grain interior. Typical initial configuration of sample II is shown in Fig. 1. Specifically, grain 4 is the reference configuration ( $X$  direction is  $[111]$  and  $Y$  direction is  $[11\bar{2}]$ ). Periodic boundary conditions are applied in all three directions. In the present simulations, about 536 000 atoms are contained in each of these three samples. An empirical embedded-atom method (EAM) potential developed by Mishin *et al.*<sup>24</sup> is used in the present study, which is calibrated according to the *ab initio* values of stacking fault and twin formation energies.<sup>24</sup>

<sup>a)</sup>Electronic mail: [chaoajing@lnm.imech.ac.cn](mailto:chaoajing@lnm.imech.ac.cn)

<sup>b)</sup>Electronic mail: [ywei@lnm.imech.ac.cn](mailto:ywei@lnm.imech.ac.cn)

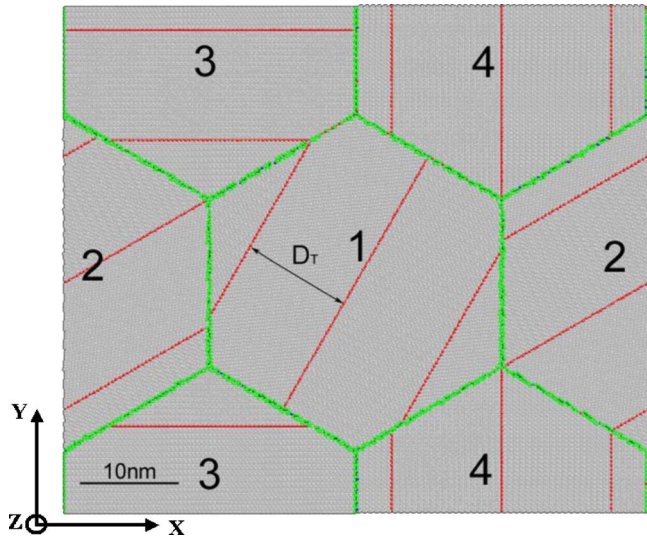


FIG. 1. (Color online) Typical initial configuration of nc Cu with ultrathin lamella twins (sample II). Periodic boundary conditions are used in all three dimensions. Atoms are colored according to common neighbor analysis.  $D_T$  is the twin lamella spacing (TLS).

For the purpose of viewing defects in the samples, colors are assigned to the atoms according to a local crystallinity classification visualized by common neighbor analysis,<sup>25</sup> which permit the distinction between atoms in a local hexagonal-close-packed (hcp) environment and those in a fcc environment. Gray stands for fcc atoms, red for hcp atoms, green for other 12-coordinated atoms, and blue for the non-12-coordinated atoms. A single line of hcp atoms represents a TB, two adjacent hcp lines stand for an intrinsic stacking fault, and two hcp lines with a fcc line stand for an extrinsic stacking fault between them.

The simulated samples are firstly relaxed in the isobaric-isothermal ensemble under both the pressure 0 bar and temperature 300 K for 20 ps. After equilibration processes, simulations start under the constant strain rate condition. The Melchionna equation of motion for the NPT ensemble governs the dynamics of the system, using a combination of a Nosé-Hoover thermostat and a Parrinello-Rahman barostat.<sup>26,27</sup> A constant strain rate is adopted in the X direction and both boundary conditions in Y and Z directions are specified as stress-free. Strain is introduced by uncoupling the unit cell vector along the X direction from the dynamics and extending it during the simulation according to the applied strain rate. This is the same method used in Refs. 21, 28, and 29.

### III. SIMULATION RESULTS AND DISCUSSIONS

Figure 2 shows the typical tensile stress-strain curves at  $T=300$  K under a constant strain rate of  $2 \times 10^8 \text{ s}^{-1}$  for the three samples. All the three samples show a nearly linear stress-strain response up to a strain about 0.5%. Elastic Young's moduli extracted from the curves are the same for the three samples, which are about 110 GPa. The flow stresses, estimated by averaging the tensile stress from a strain  $\varepsilon=0.02$  to 0.12, are 2.8, 2.5, and 2.1 GPa for samples I, II, and III, respectively.

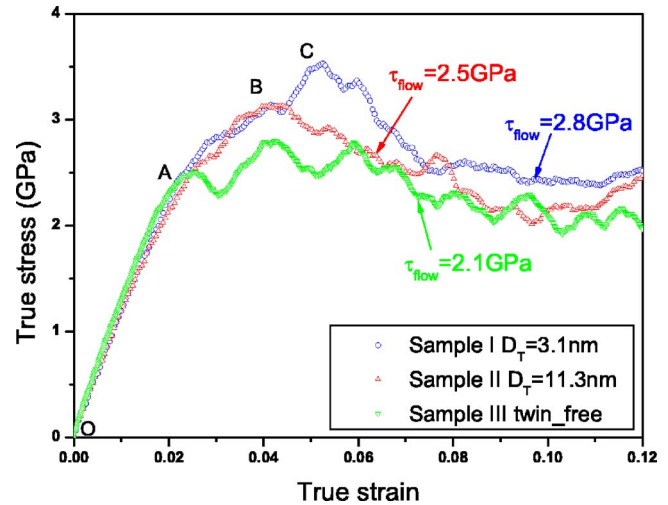


FIG. 2. (Color online) Stress-strain ( $\sigma$ - $\varepsilon$ ) curves for the three samples under uniaxial tensile loading strain rate of  $2 \times 10^8 \text{ s}^{-1}$  and 300 K temperature. Flow stress is calculated by averaging tensile stresses from strain  $\varepsilon = 0.02$  to 0.12.

By monitoring the deformation snapshots, we observe that the onsets of plasticity via the emission of first individual partial dislocation from grain boundaries (GBs) occur at the strain 1.5% and 1% for samples II and III, respectively (see Figs. 3 and 4) and the corresponding yield stresses ( $\sigma_y$ ) are 1.8 and 1.0 GPa (see Fig. 2). The fact that both the yield stress and the flow stress of nanotwinned Cu are higher than that of the twin-free case suggests that TBs have strengthening effects on the nc Cu.

Figure 3 shows the snapshots of uniaxial tensile deformation of twin-free sample. For the twin-free sample, plastic deformation is initially originated via the nucleation of partial dislocation from GBs at a strain of 1%, and then a large number of partial dislocations are emitted from GBs and slip across the whole grains. All the dislocations are the  $1/6[112]$

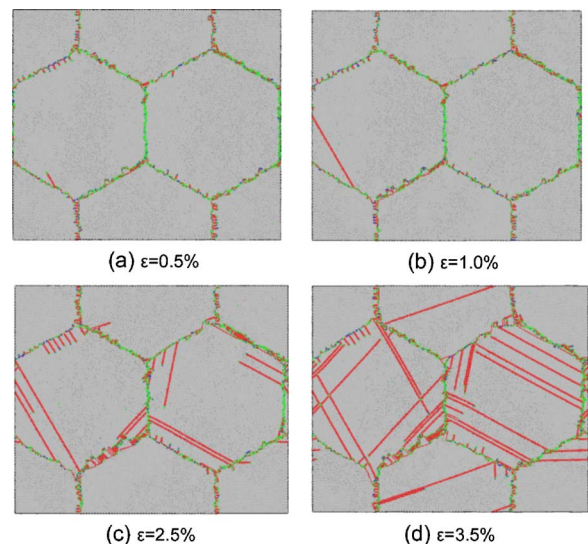


FIG. 3. (Color online) Snapshots of uniaxial tensile deformation of twin-free sample. (a) Elastic deformation. (b) The first partial dislocation nucleated from GBs at strain of 1.0% is observed. (c) Large number of dislocations slip across the whole grains and stacking faults left behind. (d) Cross-slip of stacking faults.



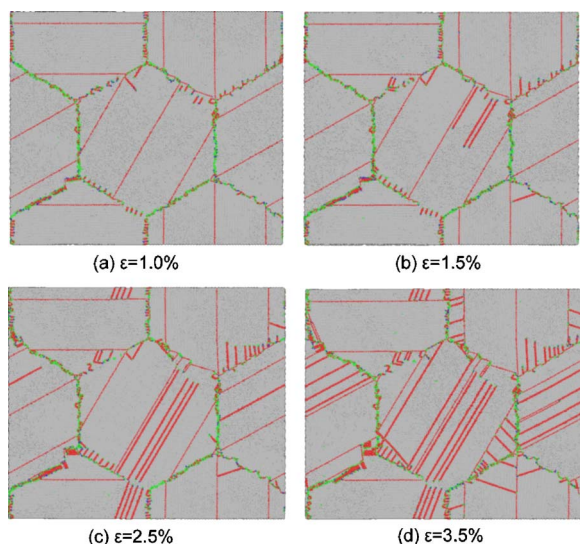


FIG. 4. (Color online) Snapshots of uniaxial tensile deformation of nanotwinned sample (sample II). (a) Elastic deformation. (b) The first partial dislocations nucleated from GBs at strain of 1.5% is observed. [(c) and (d)] large number of dislocation slip and then blocked by TBs.

Shockley partial dislocations as evidence that stacking faults leave behind the leading partial dislocations [see Figs. 3(c) and 3(d)]. The observation of no trailing partial dislocations nucleated from GBs during deformation is in agreement with the work of Swygenhoven *et al.*,<sup>18</sup> in which the authors argued that the extended partial dislocations are the predominant mode of plastic deformation mechanism for those metals that have the ratio of the unstable to intrinsic stacking fault energy much larger than unity (the ratio is 3.56 for Mishin Cu EAM potential<sup>24</sup>). The continuous process of partial dislocation nucleation from the GBs and annihilation in the GBs at the opposite ends of the grains results in a number of stacking faults left in the grains [see Figs. 3(c) and 3(d)].

Figure 4 shows the typical snapshots of uniaxial tensile deformation of nanotwinned sample (sample II). The undeformed nanotwinned Cu sample is dislocation-free in the grains. Under tensile loading, initial plastic deformation occurs via the nucleation of partial dislocations from GBs at a strain of 1.5%. When the dislocations move and meet with TBs, the movement of dislocations is blocked by the TBs

[see Figs. 4(c) and 4(d)]. These observations clearly illustrate that the presence of TBs effectively affects the plastic deformation mechanism of nc materials.

Obviously, TLS plays a significant role in determining the strength of the nc Cu. The sample with small TLS shows higher yield stress and flow stress compared with the sample with large TLS (see Fig. 2). Higher density of twin lamina has larger volume fraction of TBs, which makes the TBs more effective in strengthening the materials. The stress-strain curve of Cu with high density twins becomes quite flat after the initial few percent of plastic strain, with high strain hardening rate only in the early stage of plastic deformation. In this manner, strain hardening can be rationalized as the accumulation of dislocations at the TBs which makes further deformation harder; therefore larger stress is required to continue further plasticity.

In order to further elucidate that TLS has an important impact on strengthening effects, we also compare the dislocation density of the three samples at the same deformation strain 0.05. Abundant dislocations are detected at the TBs in the small TLS (sample I) [see Fig. 5(a)], while relatively small amounts of dislocations are trapped in the grain interior of the large TLS (sample II) [see Fig. 5(b)]. As for the twin-free (sample III), dislocations glide freely across the whole grain without block as nearly no dislocations are detected in the grain interior, only leaving stacking faults behind and deformation twins [see Fig. 5(c)].

Here we predict that TB interface can also be served as dislocation nucleation sites when the coherent TBs gradually lose coherency. Figure 6 shows the consecutive snapshots of the nucleation of dislocation from TBs. As can be seen, a unit  $1/2[110]$  dislocation is nucleated from TB, and then it dissociates into two partial dislocations, a  $1/3[111]$  Frank partial dislocation left at TB and a  $1/6[11\bar{2}]$  Shockley partial dislocation propagated into the grain interior [see Fig. 6(a)]. After 25 ps, the Shockley partial dislocation is blocked by another TB. At the same time, another partial dislocation nucleated from other TB sites is observed [see Fig. 6(b)]. This means that with dislocations deposited on TB interfaces, the coherent TBs gradually lose coherency and could be ready for dislocation nucleation sites. The extremely high shear stress in the grains facilitates this type of dislocation

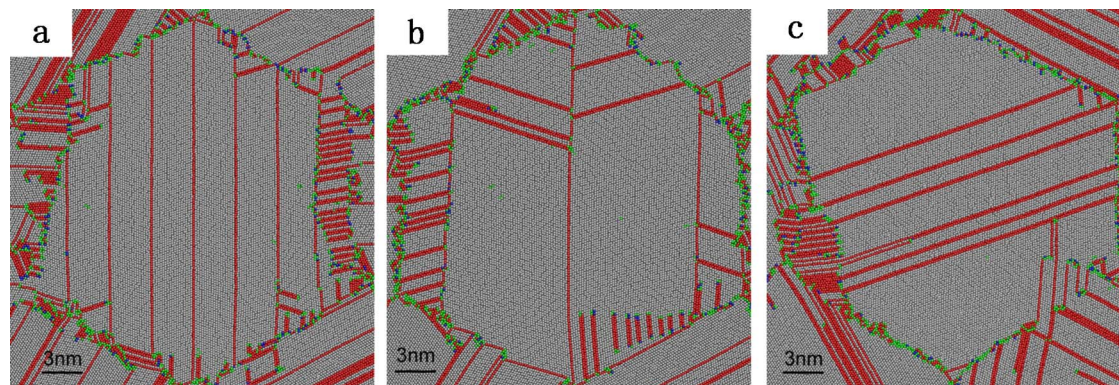


FIG. 5. (Color online) Deformation snapshots of three samples at the same strain 0.05 loaded at a strain rate of  $\dot{\epsilon}=2 \times 10^8 \text{ s}^{-1}$  and 300 K temperature. (a) Abundant dislocations trapped by TBs and some transmitted across TBs are observed in the small TLS sample. (b) Small amount of dislocations are detected in the large TLS sample. (c) Partial dislocations move across the whole grain and then stacking faults and deformation twins left within the twin-free sample.

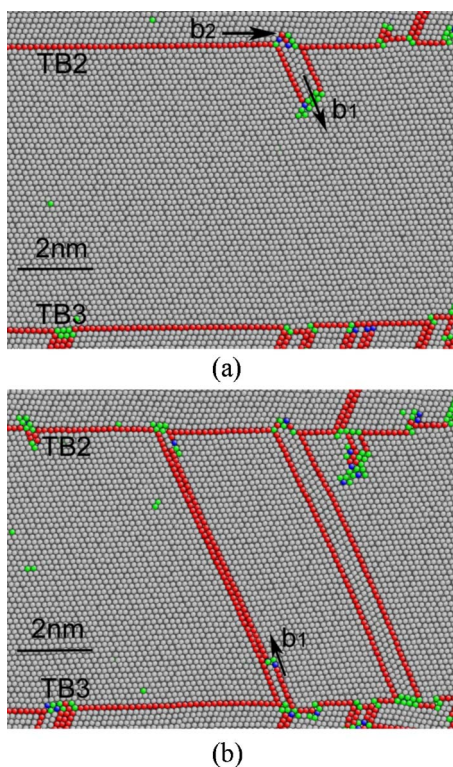


FIG. 6. (Color online) The nucleation and propagation of dislocations from TBs. (a) A unit  $1/2[110]$  dislocation nucleated from TB2 and then dissociated into two partial dislocations, a Frank partial dislocation  $b_2=1/3[111]$  and a Shockley partial dislocation  $b_1=1/6[11\bar{2}]$  is observed. (b) After 25 ps, the Shockley partial dislocation propagates and then blocked by TB3, at the same time another partial dislocation nucleated from TB3 is observed.

nucleation mechanism. These observations are also indicated by postindentation transmission electron microscope (TEM) image.<sup>6</sup> The mechanism of dislocation nucleation from TBs would influence the stress-strain response and may contribute to plastic deformation, which is analogous to conventional GBs in the nc Cu. Also, there are some partial dislocations transmitted across the TBs, which would require a stress concentration at the twin/slip band intersection.<sup>8</sup> The interaction between dislocation and TBs is of great importance in characterizing the mechanical behavior of nc materials with high density of twin lamella. Recently, Zhu *et al.*<sup>30</sup> has found that TB-mediated slip transfer reactions are rate controlling by using atomistic reaction pathway calculations. They attributed the relatively high ductility of nanotwinned copper to the hardenability of TBs as TBs gradually lose coherency during deformation. We note that the migration of preexisting TBs (Ref. 13) by means of partial dislocations slip on the  $\{111\}$  glide plane adjacent to the TBs is not the dominant plastic deformation mechanism in the nanotwinned Cu as compared with that in the nanotwinned Al reported previously,<sup>12,13</sup> also for the different relative values of the extrema of the generalized planar fault energy curves.

In conventional ways, the strength of the materials can be increased by grain refinement, which is the well-known Hall-Petch effect. The introduction of nanoscale twins into the submicrograins is also an effective means to improve the strength of metals for TB is a special GB with low GB energy. The microscopic mechanism of strain hardening effects

can be understood by considering the TBs as barrier to the movement of dislocations. The similar idea is also manifested by both our atomistic simulations of twinned Cu nanowires<sup>6</sup> and postmortem TEM observation of nanotwinned Cu.<sup>1,8</sup>

It was thought that the primary reason for conventional CG materials early necking and failure was attributed to the plastic deformation instability.<sup>7</sup> While the nanotwinned Cu has high strain hardening rate and can prevent large deformation in local regions. Meanwhile, dislocation accumulation in the twin lamella structures is expected to be an effective way of improving strength of materials while not depressing the elongation ductility.<sup>7</sup> Since GBs always serve as both source and sink of dislocations,<sup>17</sup> dislocations are not easily trapped inside in twin-free Cu sample as they are readily for getting incorporating into the near GBs a short distance away, therefore hardening mechanism in terms of conventional dislocation pile-up on the GBs is not seen in tens nanometer grain size samples. In contrast, it is an effective means for TBs preventing dislocation movements and thus leads to strain hardening and improves the necking instability. Furthermore, one kind of key differences between the structure of perfect TB interfaces and GBs is that nanovoids (or nanoporous) inevitably existed in the GBs, which would severely influence ductility of nc metals, while in contrast, perfect structure of coherent TBs without these defects only strengthen the materials while not sacrificing ductility of materials. The bimodal structure of coherent TBs embedded in the matrix of the large grain size,<sup>7</sup> taking the profit of both the TB strengthen effects and the feature of GBs providing dislocation sources, has shown to be a potential strategy to sustain both high strength and ductility of pure metals. On the other hand, GB mediated plasticity in terms of GB sliding and grain rotation may result in defects (nanoporous and nanocracks) at GBs and would consequently ruin ductility. By contrast, the facts of coherent TBs have very lower GB energy and the properties of resisting sliding could benefit to tensile ductility. We note that the presence of nanosized twins not only take effects on mechanical properties of bulk metals but also on metallic nanowires.<sup>6</sup>

Because of the short time scale accessible to the MD simulations with recent computational resource, ultrahigh strain rate is used in the simulations to obtain the required strain for plastic deformation. The calculated flow stresses are thus obtained several orders of magnitude higher than that of experiments. To investigate the strain rate sensitivity of these samples, we have performed MD simulations on these three simulated samples at different strain rates. Figure 7 shows the stress-strain curves for twin-free (sample III) [Fig. 7(a)] and nanotwinned (sample I) [Fig. 7(b)] at different strain rates. A factor of 5 reduction of the strain rate thus results in a 10% reduction in the flow stress. This is consistent with previous MD calculations.<sup>20,21</sup> Noted that at the same high strain rate, the flow stress difference between the nanotwinned and twin-free samples is not changed, which is clear a evidence that TBs play significant role in strengthening of Cu with fixed grain size.



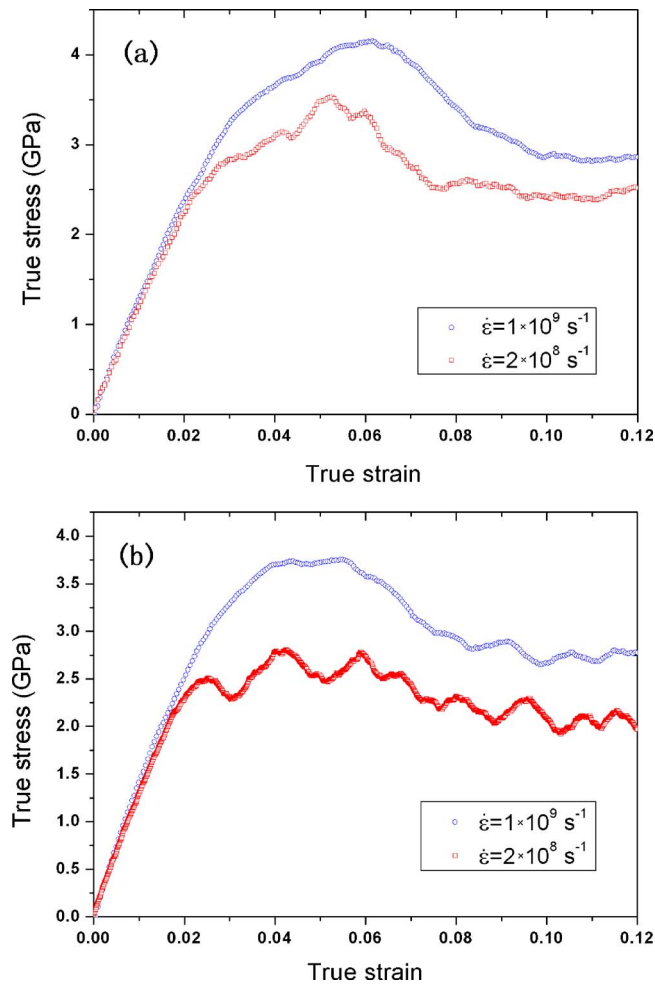


FIG. 7. (Color online) Stress-strain curves at different strain rates for (a) nanotwinned (sample I) and (b) twin-free (sample III) samples.

#### IV. SUMMARY

In summary, in this work the uniaxial tensile behavior of bulk nc Cu with ultrathin lamella growth twins, with a highly idealized columnar geometry, has been studied by using MD simulations. The results have revealed that the plastic deformation mechanism of nc Cu with nanotwins is via the nucleation of partial dislocations from GBs, and then the further movement of the dislocations is effectively blocked by the TBs. At the initial plastic deformation stage, the abundance of TBs providing obstacles to dislocation motion leads to an enhanced strength in nanotwinned Cu. In some cases, some partial dislocations could transmit TBs, which require high stress concentration. For the samples with different TB spacing and constant grain size, the results show that the twin lamella thickness plays an important role in the strengthening effects, i.e., the thinner the thickness of the twin lamella, the harder the material. The results presented in this work are in good agreement with the experimental postmortem TEM observations and results.<sup>1,8,9</sup> In addition, we have predicted that TBs can act as dislocation nucleation sites at large strains as they gradually lose coherency during deformation.

This dislocation activity could possibly make contributions to both strength and plasticity. This atomic-level study provides quantitative and mechanistic insights into the role played by TBs, which points out that controlled introduction of nanosized twin lamella into nc or UFG metals can be an effective way of improving strength without suppression of tensile ductility.

#### ACKNOWLEDGMENTS

The authors are supported by the National Science Foundation of China through Grant Nos. 10432050, 10428207, and 10672163, and Contract No. KJCX2-YW-M04 of the Chinese Academy of Sciences. All of the calculations were performed using a modified version of PARADYN,<sup>31</sup> which is originally developed by S. Plimpton at Sandia National Laboratory.

- <sup>1</sup>L. Lu, Y. F. Shen, X. H. Chen, L. H. Qian, and K. Lu, *Science* **304**, 422 (2004).
- <sup>2</sup>X. Zhang, A. Misra, H. Wang, M. Nastasi, J. D. Embury, T. E. Mitchell, R. G. Hoagland, and J. P. Hirth, *Appl. Phys. Lett.* **84**, 1096 (2004).
- <sup>3</sup>X. Zhang, H. Wang, X. H. Chen, L. Lu, K. Lu, R. G. Hoagland, and A. Misra, *Appl. Phys. Lett.* **88**, 173116 (2006).
- <sup>4</sup>B. Wu, A. Heidelberg, J. J. Boland, J. E. Sader, X. M. Sun, and Y. D. Li, *Nano Lett.* **6**, 468 (2006).
- <sup>5</sup>A. J. Cao and Y. G. Wei, *Phys. Rev. B* **74**, 214108 (2006).
- <sup>6</sup>A. J. Cao, Y. G. Wei, and S. X. Mao, *Appl. Phys. Lett.* **90**, 151909 (2007).
- <sup>7</sup>E. Ma, Y. M. Wang, Q. H. Lu, M. L. Sui, L. Lu, and K. Lu, *Appl. Phys. Lett.* **85**, 4932 (2004).
- <sup>8</sup>L. Lu, R. Schwaiger, Z. W. Shan, M. Dao, K. Lu, and S. Suresh, *Acta Mater.* **53**, 2169 (2005).
- <sup>9</sup>Y. F. Shen, L. Lu, Q. H. Lu, Z. H. Jin, and K. Lu, *Scr. Mater.* **52**, 989 (2005).
- <sup>10</sup>Y. F. Shen, L. Lu, M. Dao, and S. Suresh, *Scr. Mater.* **55**, 319 (2006).
- <sup>11</sup>R. J. Asaro and S. Suresh, *Acta Mater.* **53**, 3369 (2005).
- <sup>12</sup>A. G. Frøseth, P. M. Derlet, and H. Van Swygenhoven, *Appl. Phys. Lett.* **85**, 5863 (2004).
- <sup>13</sup>A. G. Frøseth, H. Van Swygenhoven, and P. M. Derlet, *Acta Mater.* **52**, 2259 (2004).
- <sup>14</sup>Z. H. Jin, P. Gumbsch, E. Ma, K. Albe, K. Lu, H. Hahn, and H. Gleiter, *Scr. Mater.* **54**, 1163 (2006).
- <sup>15</sup>V. Yamakov, D. Wolf, S. R. Phillpot, A. K. Mukherjee, and H. Gleiter, *Nat. Mater.* **1**, 1 (2002).
- <sup>16</sup>V. Yamakov, D. Wolf, S. R. Phillpot, A. K. Mukherjee, and H. Gleiter, *Nat. Mater.* **3**, 43 (2004).
- <sup>17</sup>H. Van Swygenhoven, *Science* **296**, 66 (2002).
- <sup>18</sup>H. Van Swygenhoven, P. M. Derlet, and A. G. Frøseth, *Nat. Mater.* **3**, 399 (2004).
- <sup>19</sup>H. Van Swygenhoven, P. M. Derlet, and A. G. Frøseth, *Acta Mater.* **54**, 1975 (2006).
- <sup>20</sup>J. Schiøtz and K. W. Jacobsen, *Science* **301**, 1357 (2003).
- <sup>21</sup>J. Schiøtz, *Scr. Mater.* **51**, 837 (2004).
- <sup>22</sup>T. Shimokawa, A. Nakatani, and H. Kitagawa, *Phys. Rev. B* **71**, 224110 (2005).
- <sup>23</sup>V. Yamakov, D. Wolf, M. Salazar, S. R. Phillpot, and H. Gleiter, *Acta Mater.* **49**, 2713 (2001).
- <sup>24</sup>Y. Mishin, M. J. Mehl, D. A. Papaconstantopoulos, A. F. Voter, and J. D. Kress, *Phys. Rev. B* **63**, 224106 (2001).
- <sup>25</sup>J. D. Honeycutt and H. C. Andersen, *J. Phys. Chem.* **91**, 4950 (1987).
- <sup>26</sup>S. Melchionna, G. Ciccotti, and B. L. Holian, *Mol. Phys.* **78**, 533 (1993).
- <sup>27</sup>S. Melchionna, *Phys. Rev. E* **61**, 6165 (2000).
- <sup>28</sup>A. J. Cao and Y. G. Wei, *Appl. Phys. Lett.* **89**, 041919 (2006).
- <sup>29</sup>A. J. Cao and Y. G. Wei, *Phys. Rev. B* **76**, 024113 (2007).
- <sup>30</sup>T. Zhu, J. Li, A. Samanta, H. G. Kim, and S. Suresh, *Proc. Natl. Acad. Sci. U.S.A.* **104**, 3031 (2007).
- <sup>31</sup>S. J. Plimpton, *J. Comput. Phys.* **117**, 1 (1995).